Optically Compensated Bend Cell with Pixel-Isolating Polymer Wall for a Flexible Display Application

Seong Ryong Lee**, Joong Ha Lee**, Hong Jeek Jang**, Tae-Hoon Yoon*, and Jae Chang Kim*

Abstract

We demonstrate an optically compensated bend (OCB) cell with pixel-isolating polymer wall. The polymer wall is formed by anisotropic phase separation of LCs and UV-curable polymer. The fabricated cell is initially in π-twisted state so that it shows uniform and fast bend transition without any transition nucleus. The proposed cell has lower driving voltage than conventional OCB cell. Also, the polymer wall provides mechanical stability, hence preventing distortion of display image from external pressure.

Keywords : Optically compensated bend, Polymer wall, Bend transition, Driving voltage, Mechanical stability

1. Introduction

Due to its rapid switching and wide viewing angle properties, optically compensated bend (OCB) mode liquid crystal (LC) display (LCD) [1-4] has attracted a fair amount of attention as one of the candidates for many portable display applications such as mobile phone, portable multimedia players and car-navigations.

An OCB cell is composed of a pi cell and some retardation films. The pi cell has the fastest response speed among all nematic LC modes as the switching does not involve backflow [1]. Moreover, the pi cell can obtain high contrast ratio and wide viewing angle property by using retardation films [2-4]. A pi cell is made by sandwiching LC molecules between two parallel-aligned substrates. The LC molecules in the pi cell should be bend-aligned for high speed operation. However, as the initial stable state of the conventional pi cell with a low pretilt angle is splay state, the splay state has to be changed to a bend state. This transition from the splay state to the bend state is nontrival phenomenon due to the topological difference between the two states.

Recently, to achieve a uniform and fast bend transition, a polymer-induced structure of pi cell was proposed, which employed polymer network in each pixel [5]. Moreover, the polymer network is expected to prevent the deformation of an LC texture from an external pressure or bending. However, those cells demonstrated poor transmittance and contrast ratio due to index mismatching between the LCs and polymers. They showed slower on-off response time than conventional pi cell because the LC relaxation was disturbed by the polymer network within a pixel area.

Most recently, we demonstrated an initially π-twisted nematic LC (NLC) cell with pixel-isolating polymer wall by incorporating UV-curable fluorinated polymer [6]. Due to the inherent immiscible property of the fluorinated polymer, excellent anisotropic phase separation between the LCs and polymer was achieved [7]. Each pixel could be a π-twist as the initial state, so that the fabricated cell does not need any kind of nucleus which is necessary for the bend transition [6, 8]. In this paper, we demonstrate a pixel-isolated OCB cell (PI-OCB) composed of the initially π-twisted NLC cell and several retardation films which has been proposed for a wide viewing angle. Then, the electro-optical properties and enhancement of the mechanical stability were measured and compared to a conventional OCB cell.

2. Stabilization of the π-twisted state

Fig. 1 shows the fabrication process of the initially π-twisted NLC cell with the pixel-isolating polymer wall.

Manuscript received November 6, 2007; accepted for publication December 25, 2007.
This research was funded by a grant (F0004130-2007-23) from the Information Display R&D Center, one of the 21st Century Frontier R&D Program supported by the Ministry of Commerce, Industry and Energy of the Korean Government, and by a Pusan National Research Grant.
* Member, KIDS; ** Student Member, KIDS
Corresponding Author : Seong Ryong Lee
School of Electrical Engineering, Pusan National University
San 30, Jangjeon-dong, Kumjeung-gu, Busan 609-735, Korea.
E-mail : mengmol@pusan.ac.kr **Tel** : 051-510-1700 **Fax** : 051-515-5190

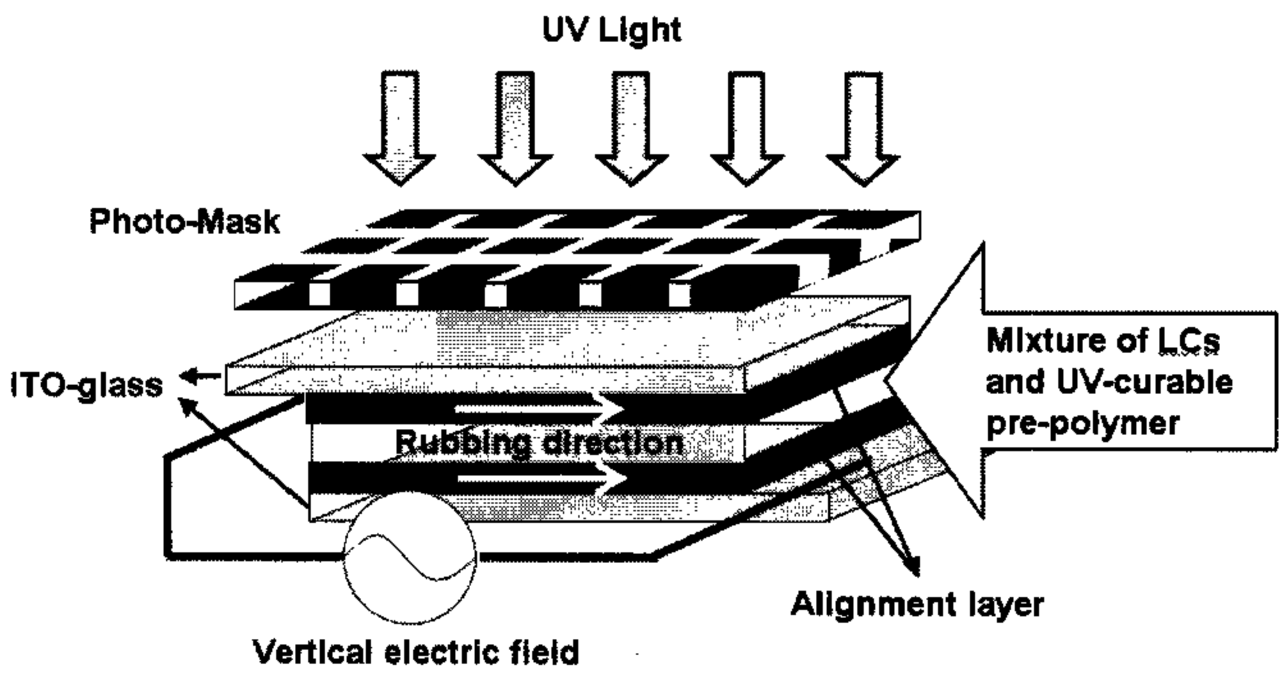

Fig. 1. Fabrication process of an initially π-twisted NLC cell.

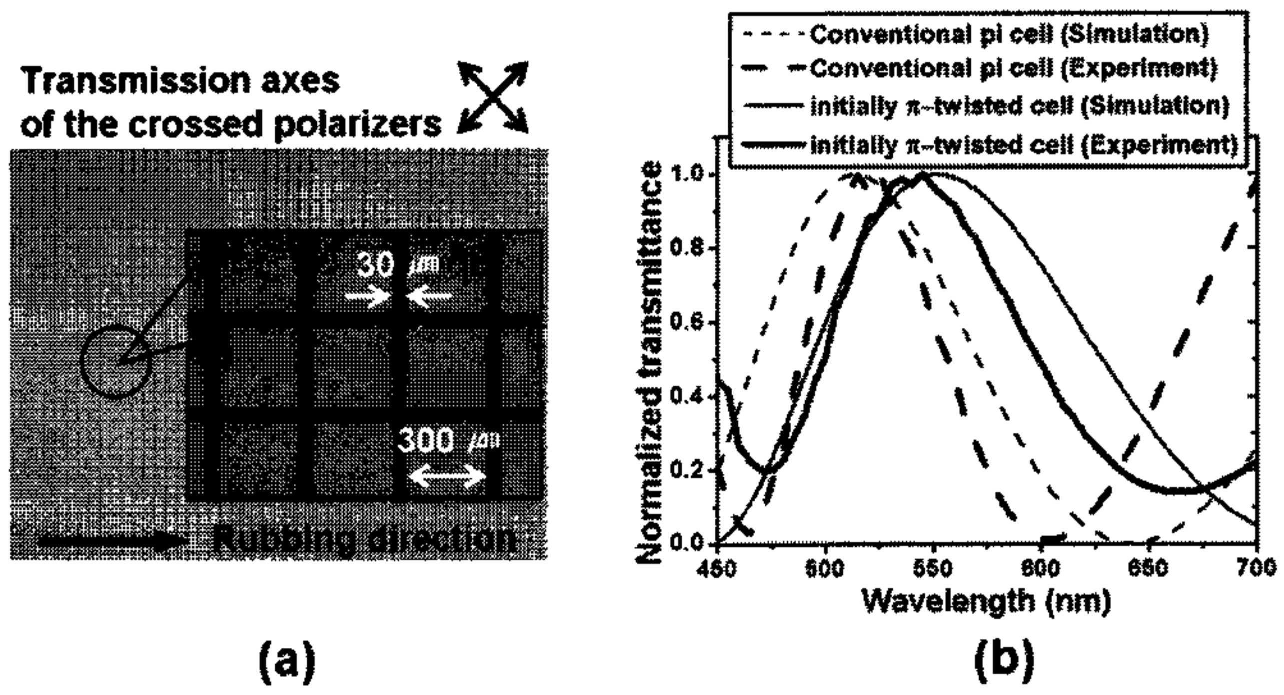

Fig. 2. (a) Images of the fabricated cell with a polarizing microscope, and (b) wavelength dispersion characteristics compared to that of the conventional pi cell.

The polymer wall was formed by a phase separation of a mixture of LCs and UV-curable pre-polymers with a 90:10 wt%. The LC and pre-polymers used in the experiment were MLC-6265-100 (Merck) and fluorinated acrylates, respectively. First, an alignment layer of AL-90101 (JSR Corp.) was spin-coated on the ITO-glass substrates. Then, the cell was assembled with parallel rubbing directions of the two substrates. The cell-gap was maintained as 5.6μm by using silica spacers. Then, the mixture of LC and pre-polymer was injected into the empty cell. To crosslink the pre-polymer and isolate a pixel, the cell was exposed to an UV light through a photo-mask. The photo-mask has dark square patterns of a 300 μm×300 μm pixel size and transparent boundaries of 30 μm. The intensity of light source was 30 mW/cm^2 and had a peak wavelength of 365 nm. During the UV light exposure, a vertical electric field (1.5 V/μm, 1 kHz) was applied between the two ITO-substrates. After the UV light exposure and formation of the polymer wall, the bend state is relaxed into the π-twisted state and stabilized as soon as the electric field is removed.

Fig. 2(a) shows the microscope images of the fabricated cell sandwiched between crossed polarizers. The light is transmitted only in the pixel region and blocked in the region of the polymer wall. It represents that the anisotropic phase separation between the LCs and pre-polymers was excellently accomplished. Fig. 2(b) shows the wavelength dispersion characteristic of the fabricated cell with zero applied voltage. The transmittance dependent on a wavelength was measured by the spectrometer, MCPD-3000 (Photal) and compared with simulation result calculated by commercial software, DIMOS (autronic-MELCHERS). The measured and calculated results were compared to those of the conventional pi cell that has the same parameters of cell-gap, alignment material and LC material as the pixel-isolated cell. The calculated LC textures of the conventional and pixel-isolated cells were splay and π-twist, respectively. In Fig. 2(b), the wavelengths that show the maximum and minimum transmittances in the experimental results almost correspond to those in the calculated one.

The stabilization of π-twisted state can be explained by the effect of polymer wall. We suppose that the polymer wall has weak anchoring and the LC molecules aligned near the polymer wall may affect the free energy density of the pixel. We calculated the energy density on the condition that the LC molecules near the polymer wall aligned parallel to the polymer wall and compared it with that of a conventional pi cell as shown in Fig. 3. The horizontal and vertical axes indicate the twist angle of the LC molecules and the normalized free energy density, respectively. Each free energy density of the splay and π-twisted states in a pixel area of pixel-isolated cell was higher and lower than those of conventional pi cell, respectively. This means that the polymer wall plays a role in decreasing the difference of

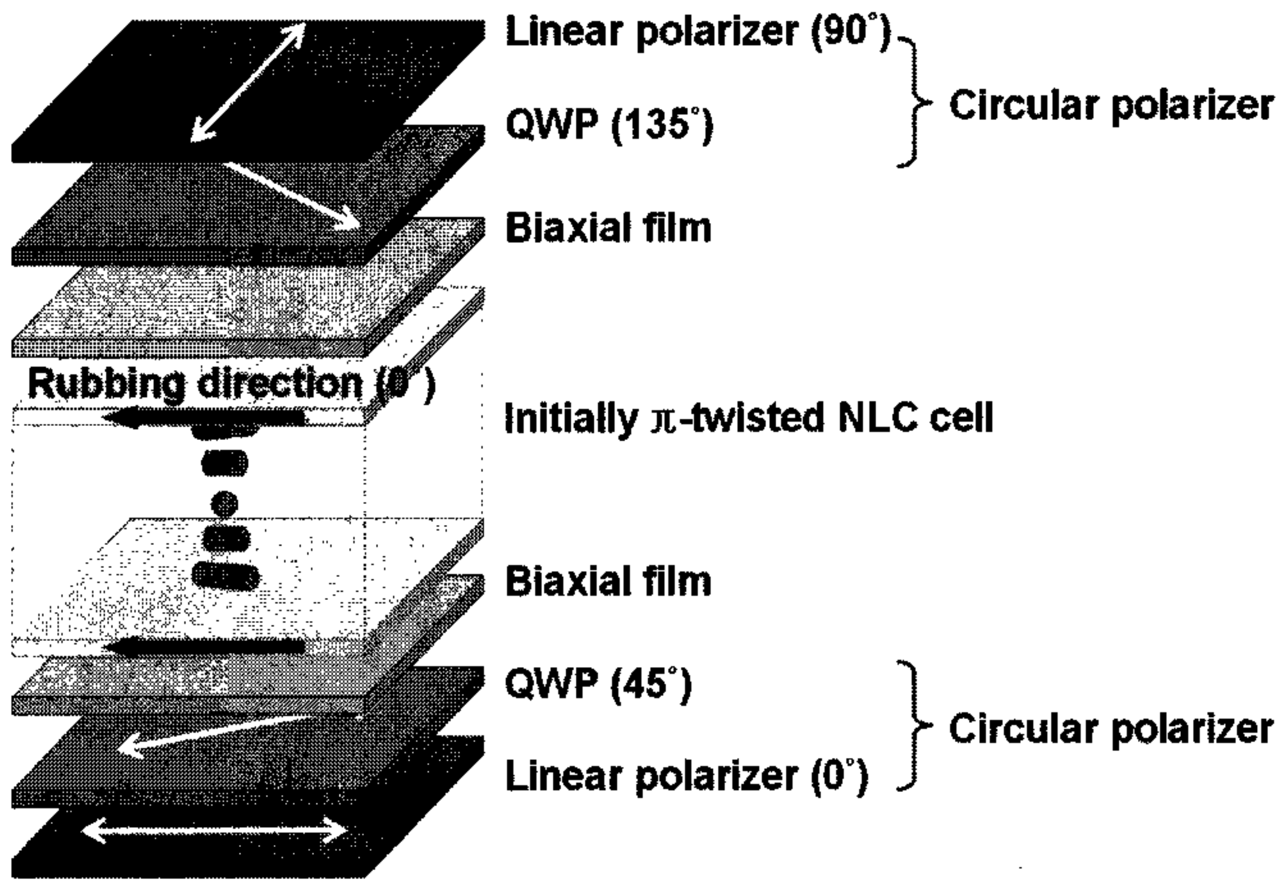

Fig. 3. Structure of the fabricated OCB cell assembled with a pi cell and optical compensation films.

free energies between the splay and π-twisted states. Therefore, it may be difficult to replace the π-twisted state to the splay state, and the π-twisted state can be stabilized.

3. Pixel-isolated optically compensated bend cell

A PI-OCB cell was assembled with the fabricated initially π-twisted NLC cell and several optical films as shown in Fig. 4. Two positive a-plates and two biaxial films were introduced to suppress the light leakage of dark state at arbitrary viewing angles [9-10]. The rubbing direction of the LC cell was parallel to the angle of 0°. The retardation value of each biaxial film was 50 nm at normal direction. The parameter, N_z, of each biaxial film was 0.147 [11]. The retardation values of biaxial films play a role to cancel out the residual retardation of the LC cell at dark state for the normal and oblique direction. The transmission axes of the polarizer and analyzer are set at the angle of 0° and 90°, respectively. The retardation value of each positive a-plate was 138 nm at normal direction, and the optic axes (OAs) of the lower and upper a-plates are set at the angle of 45° and 135°, respectively. The combination of the linear polarizer and the positive a-plate plays a part as a circular polarizer, and the circular polarizer has been proposed to play an important role that the biaxial films can perform their parts [10].

We measured the optical characteristics dependent on the applied voltages of the PI-OCB cells. A conventional OCB cell was also fabricated to compare with the PI-OCB cell, which is composed of the conventional pi cell and the same film-compensating scheme as the PI-OCB cell. Figs. 5(a) and 5(b) indicate the transmission characteristics dependent on the applied voltage and wavelength dispersion characteristics of fully bright and dark states in the conventional OCB and PI-OCB cells, respectively. In Fig. 5(a), the PI-OCB cell shows much lower driving voltage than that of the conventional one. The applied voltage for fully dark state of the PI-OCB cell is 7.2 V, which is almost half the value of the conventional one, 14 V. Also, the bias voltage of 2.4 V for sustaining the bend state in the PI-OCB cell is lower than 3.2 V needed in conventional one. The lower driving voltage is supposed to be caused by more decreased retardation value near the polymer wall than in the pixel region at the same applied voltage. This can be explained as follows: Firstly, the mean pretilt angle of LCs near the wall might be higher than that of the pixel region due to the weak anchoring force of the polymer wall. Secondly, LCs might be easily reoriented parallel to the electric field because the anchoring force of the wall is weak. In Fig. 5(b), the transmittance of the PI-OCB cell at the full bright state is a little lower than that of the conventional cell as 98 % at the same pixel size. The reason for the lower transmittance can be explained by that of the lower of driving voltage.

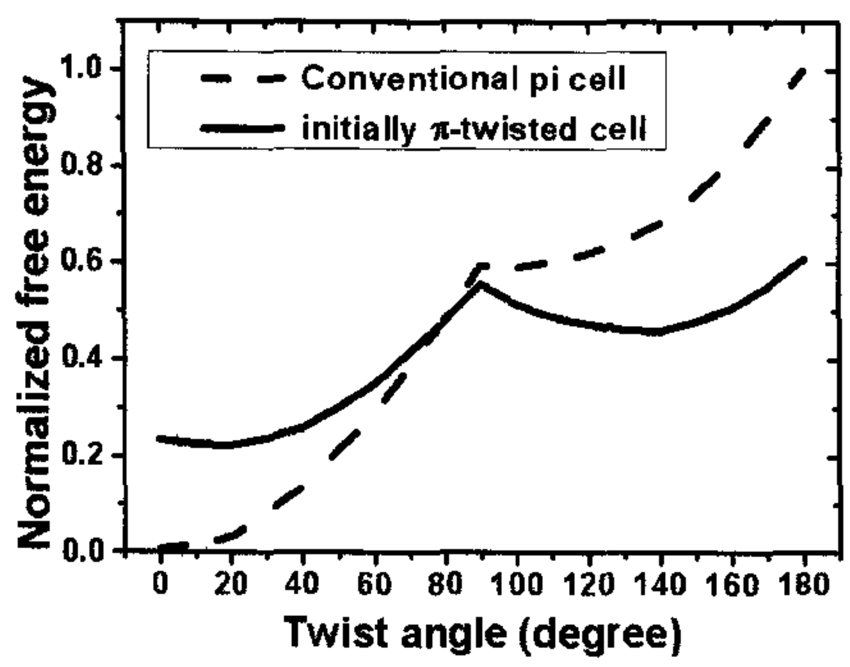

Fig. 4. Calculated free energy densities in LC cells with and without a polymer wall. In the calculation, we let the LC molecules near the polymer wall align parallel to the wall.

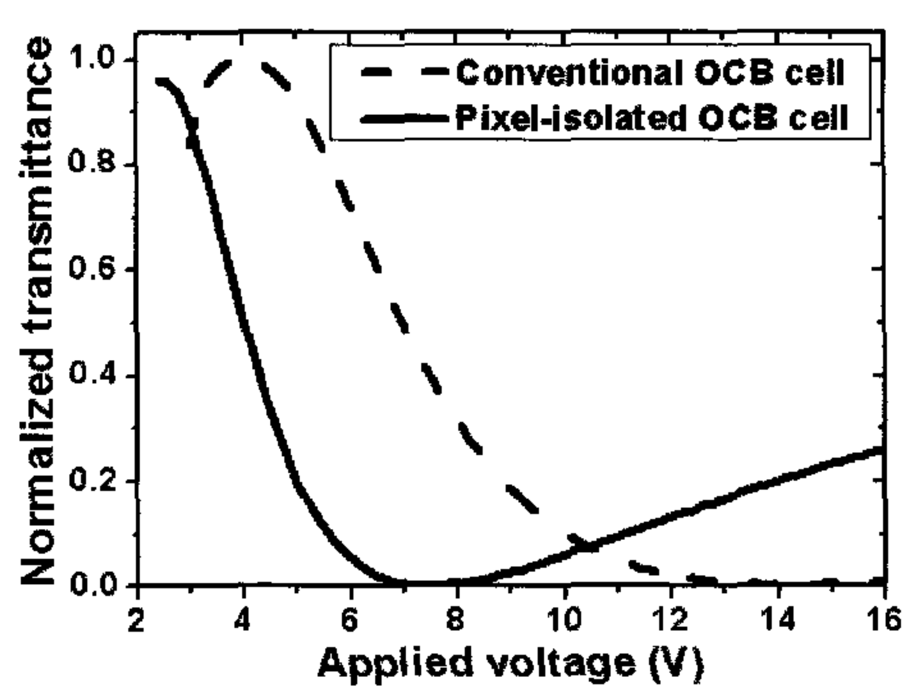

(a)

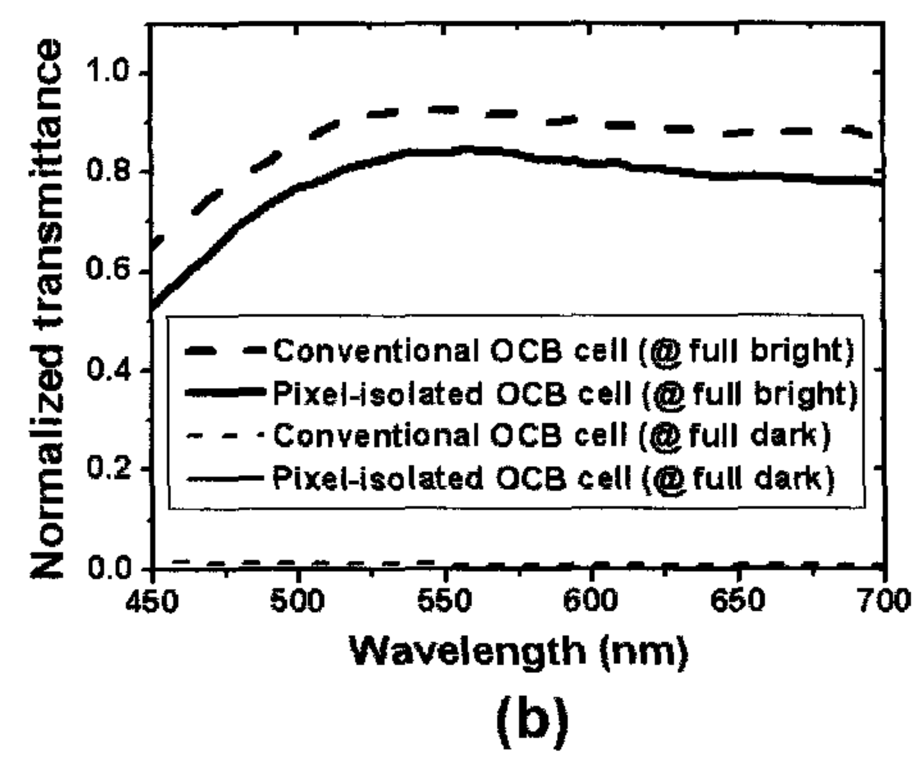

(b)

Fig. 5. (a) Transmission characteristics dependent on the applied voltage, and (b) wavelength dispersion characteristics of fully bright and dark states in the conventional OCB and PI-OCB cells, respectively.

Figs. 6(a) and 6(b) show turn-on and turn-off characteristics of the two OCB cells, respectively. In the PI-OCB cell, the response times at turn-on and turn-off were 0.68 and 2.1 ms, respectively. Those of conventional OCB cell were 0.7 and 1.8 ms, respectively. The turn-on time of the PI-OCB cell was slightly faster than that of the conventional one. In case of turn-off time, the PI-OCB cell shows slower LC relaxation than conventional one. We suppose that it is caused by the weak anchoring of the polymer wall and the relaxation is disturbed by the interaction between LC molecules and polymer wall.

Figs. 7(a) and 7(b) show simulated and measured viewing angle properties, respectively. The measured viewing angle is more than 140° (contrast ratio > 10) in both the horizontal and vertical directions, which is almost the same as that of the simulated one. Moreover, it shows a high contrast ratio of 431 at normal direction.

Finally, we tested the enhancement of the mechanical stability of the pixel-isolated cell in comparison with the conventional one. Figs. 8(a) and 8(b) show the images of the conventional OCB and PI-OCB cells with an external point pressure. The pixel-isolated cell shows much lower distortion of transmittance in comparison with conventional one by virtue of the polymer wall.

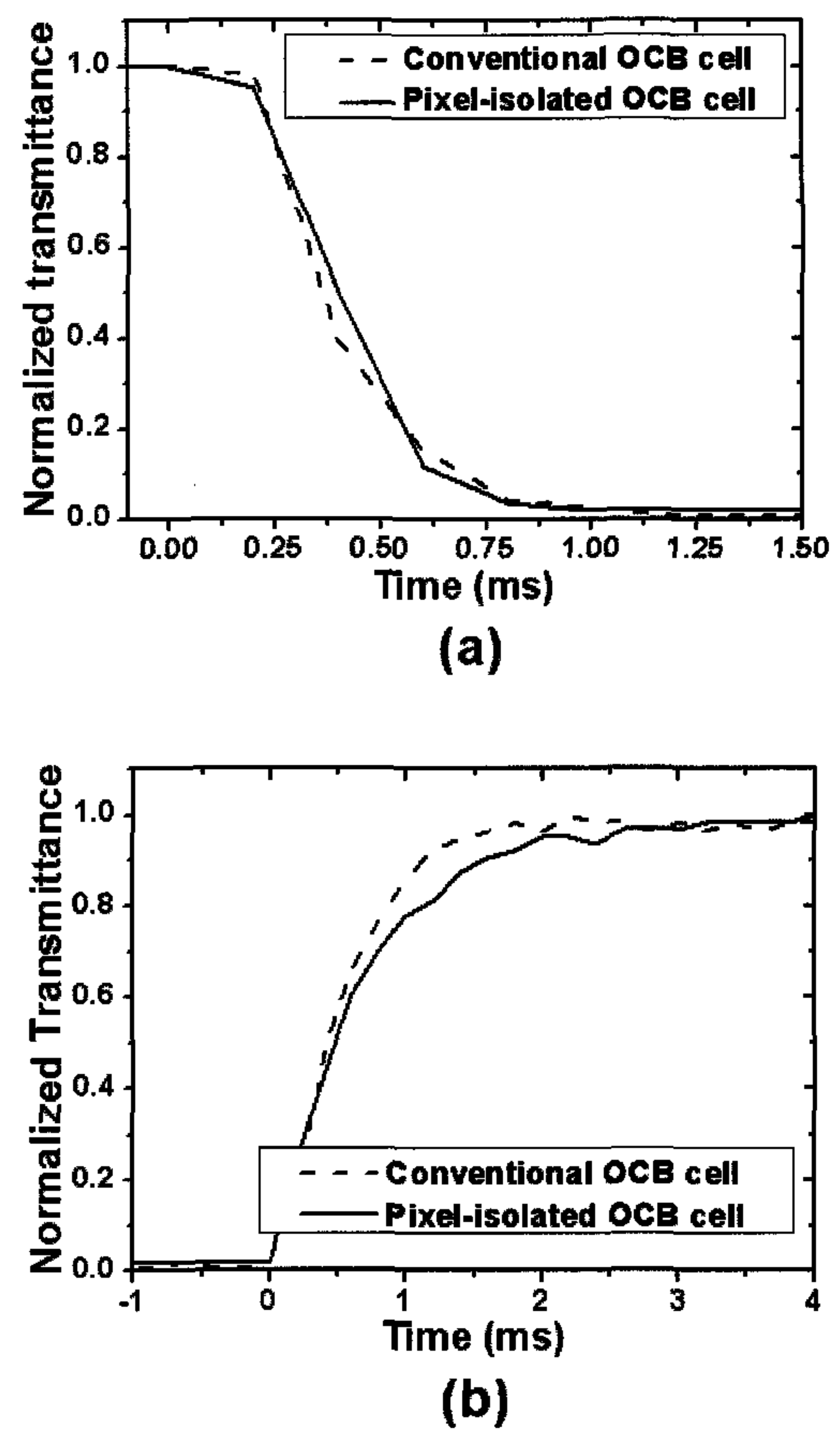

Fig. 6. Switching characteristics of the conventional OCB and PI-OCB cells: (a) turn-on time from fully dark to bright state, and (b) turn-off time from fully bright to dark state.

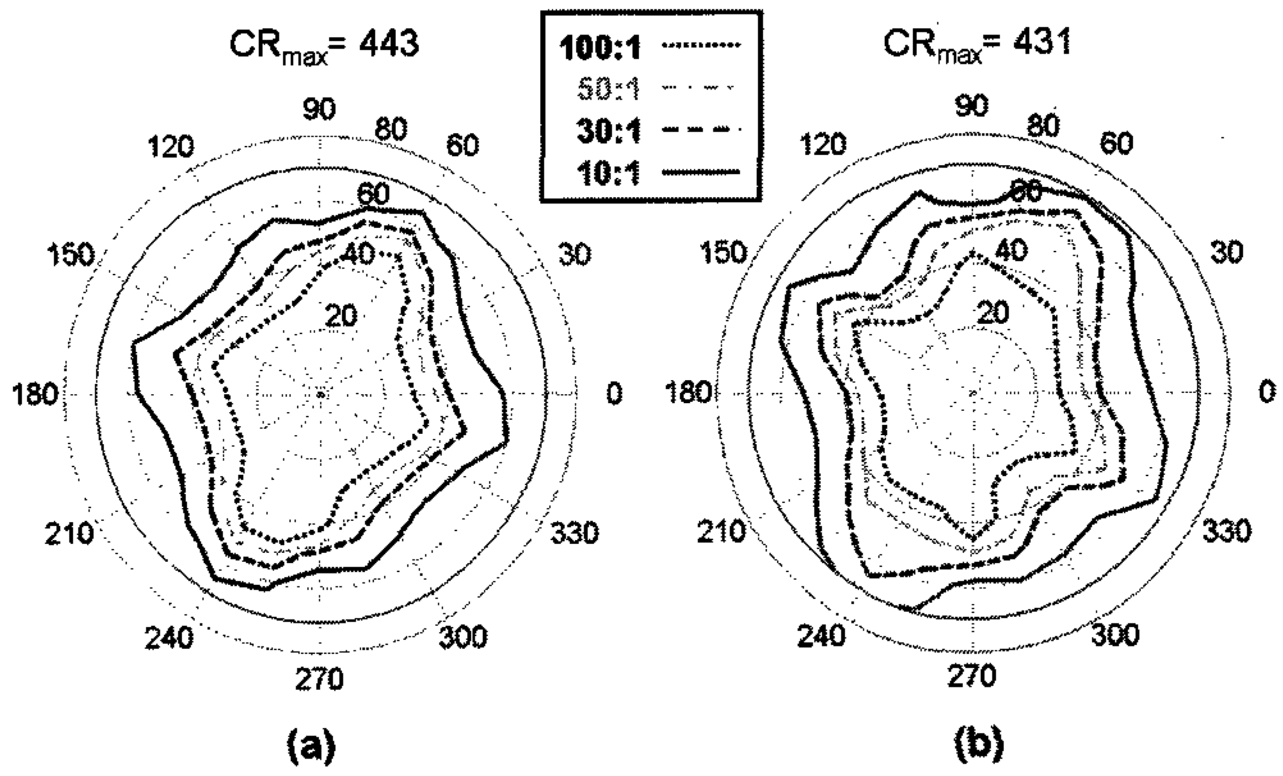

Fig. 7. Iso-contrast contours of PI-OCB cell: (a) simulated, and (b) experimental results.

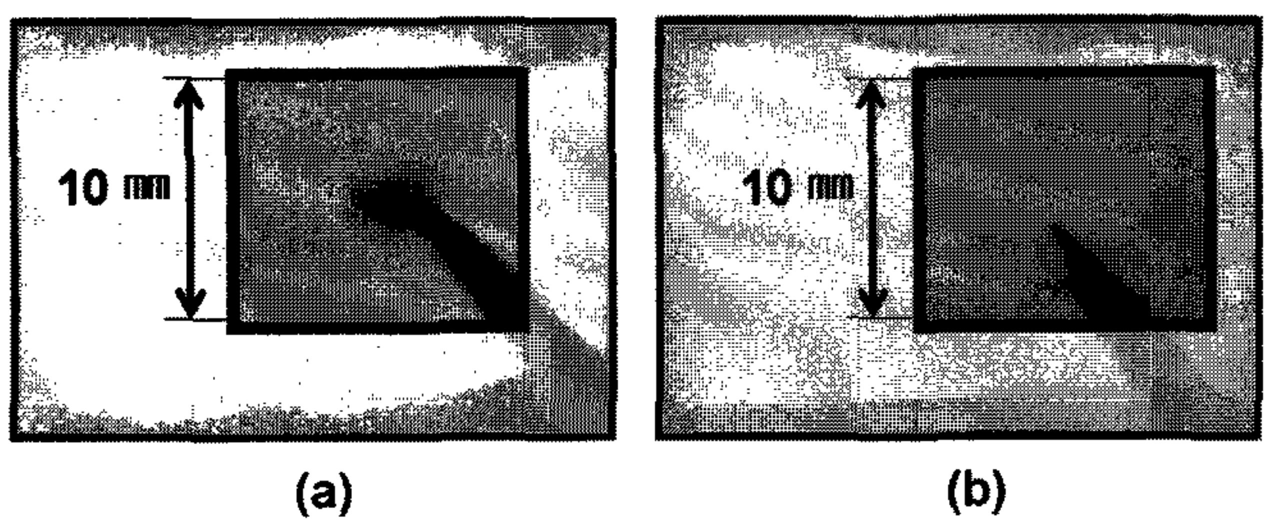

Fig. 8. Images of the (a) conventional OCB, and (b) PI-OCB cells with an external point pressure.

4. Conclusions

We proposed a PI-OCB cell which does not need any nucleus for the transition from splay to bend state. The PI-OCB cell has the advantage of lower driving voltage than that of the conventional OCB cell by the weak anchoring effect of the polymer wall. It showed high contrast ratio, wide viewing angle and fast switching properties comparable to the conventional OCB cell. Also, it showed enhanced mechanical stability which prevents distortion of a display image against external pressing. Hence the PI-OCB cell has potential applications in high speed portable LCDs as well as flexible LCDs.

References

[1] P. J. Bos and K. R. Koeler-Beran, Mol. Cryst. Liq. Cryst., **113**, 329 (1984).

[2] Miyashita, Y. Yamaguchi, and T. Uchida, Jpn. J. Appl. Phys., **34**, L177 (1995).

[3] C. L. Kuo, T. Miyashita, T. Suzuki, and T. Uchida, Appl. Phys. Lett., **68**, 1461 (1996).

[4] H. Mori and P. J. Bos, Jpn. J. Appl. Phys., Part 1 **38**, 2837 (1999).

[5] S. H. Kim and L.-C. Chien, Jpn. J. Appl. Phys., **43**, 7643 (2004).

[6] S. R. Lee, J. H. Shin, J.-I Baek, M.-C Oh, T.-H. Yoon, and J. C. Kim: Appl. Phys. Lett., **90** (2007) 163513.

[7] J.-I. Baek, J.-H. Shin, M.-C. Oh, J. C. Kim, and T.-H. Yoon, Appl. Phys. Lett., **88**, 161104 (2006).

[8] S. H. Lee, S. H. Hong, J. D. Noh, H. Y. Kim, and D.-S. Seo, Jpn. J. Appl. Phys., **40**, L389 (2001).

[9] T. Ishinabe, T. Miysahita, and T.Uchida: SID Int. Symp. Dig. Tech., (2004), p. 638.

[10] S. R. Lee, C.-G. Jhun, T.-H. Yoon, J. C. Kim, J. D. Noh, D. H. Suh, and J. Y. Lee: IMID Tech. Dig., (2005), p. 345.

[11] Y. Fujimura, T. Nagatsuka, H. Yoshimi, and T. Shimomura: SID Int. Symp. Dig. Tech., (1991), p. 739.